

The high-energy anomaly in ARPES spectra of the cuprates—many body or matrix element effect?

E. D. L. Rienks,¹ M. Ärrälä,² M. Lindroos,² F. Roth,³ W. Tabis,^{4,5} G. Yu,⁴ M. Greven,⁴ and J. Fink⁶

¹ *Helmholtz-Zentrum Berlin, Albert-Einstein-Strasse 15,*

D-12489 Berlin, Germany

² *Department of Physics,*

Tampere University of Technology,

PO Box 692, FIN-33101 Tampere, Finland

³ *Center for Free-Electron Laser Science / DESY,*
Notkestrasse 85, D-22607 Hamburg, Germany

⁴ *School of Physics and Astronomy,*

University of Minnesota,

Minneapolis, Minnesota 55455, USA

⁵ *AGH University of Science and Technology,*

Faculty of Physics and Applied Computer Science,
30-059 Krakow, Poland

⁶ *Leibniz-Institute for Solid State and Materials Research Dresden,*
P.O.Box 270116, D-01171 Dresden, Germany

(Dated: August 14, 2018)

We used polarization-dependent angle-resolved photoemission spectroscopy (ARPES) to study the high-energy anomaly (HEA) in the dispersion of $\text{Nd}_{2-x}\text{Ce}_x\text{CuO}_4$, ($x = 0.123$). We have found that at particular photon energies the anomalous, waterfall-like dispersion gives way to a broad, continuous band. This suggests that the HEA is a matrix element effect: it arises due to a suppression of the intensity of the broadened quasi-particle band in a narrow momentum range. We confirm this interpretation experimentally, by showing that the HEA appears when the matrix element is suppressed deliberately by changing the light polarization. Calculations of the matrix element using atomic wave functions and simulation of the ARPES intensity with one-step model calculations provide further proof for this scenario. The possibility to detect the full quasi-particle dispersion further allows us to extract the high-energy self-energy function near the center and at the edge of the Brillouin zone.

PACS numbers: 74.25.Jb, 74.72.Ek, 79.60.āĹŠi

One of the unique assets of angle-resolved photoemission spectroscopy (ARPES) is the ability to determine the spectral function $A(\omega, \mathbf{k})$ in energy and momentum space. The finite width and deviation of the dispersion from that calculated in an independent particle model are interpreted in the majority of cases in terms of many-body effects [1]. In the cuprate high- T_c superconductors, various kinks in the dispersion have been discovered which were analyzed in terms of a coupling of the charge carriers to bosonic excitations possibly mediating high- T_c superconductivity in these materials. Besides the kinks in the low binding energy (E_B) region ($E_B \leq 0.1$ eV) at $E_B = E_H \gtrsim 0.3$ eV the band appears to bend sharply and seems to proceed almost vertically towards the valence bands. This phenomenon has been termed "waterfall" or high-energy anomaly (HEA) [2]. The HEA has been observed in undoped cuprates [3] as well as in their hole-doped [2, 4–13], and electron-doped derivatives [4, 13–15]. In the latter two systems E_H shows a d -wave momentum dependence being larger along the nodal direction and smaller near the antinodal point opposite to the momentum dependence of the d -wave superconducting gap [6, 12, 14]. The values of E_H exhibit

a difference of ≈ 0.4 eV between hole doped and electron doped cuprates [4]. This difference was interpreted in terms of a shift of the chemical potential [14]. The experimental studies were accompanied by numerous theoretical papers [16–31].

For the phenomenon of the HEA, a number of explanations have been suggested including Mott-Hubbard models with a transition from the coherent quasi-particle dispersion to the incoherent lower Hubbard band [5, 18, 21, 26, 32], a disintegration of the low-energy branch into a holon and spinon band due to a spin charge separation [2], a coupling to spin fluctuations [9, 17, 19, 29, 33], a coupling to phonons [7], string excitations of spin-polarons [32], a bifurcation of the quasi-particle band due to an excitation of a bosonic mode of charge $2e$ [22], and a coupling to plasmons [16]. These are all intrinsic interpretations in terms of many-body interactions leading to a change of the spectral function.

However, the spectral function can strictly only be inferred from ARPES with a detailed knowledge of the photoexcitation matrix element, since the measured photocurrent is given by [1]:

$$I(\omega, \mathbf{k}) \propto |M(\omega, \mathbf{k})|^2 A(\omega, \mathbf{k}) \quad (1)$$

where the matrix element

$$M(\omega, \mathbf{k}) = \langle f | \mathbf{e} \mathbf{r} | i \rangle \quad (2)$$

is determined by the final state $\langle f |$, the initial state $| i \rangle$, and the dipole operator $\mathbf{e} \mathbf{r}$ (\mathbf{e} is the unit vector along the polarization direction of the photons).

Some ARPES studies pointed out that extrinsic effects due to matrix element effects may explain the HEA [8, 10, 12] since changes of the waterfall-like dispersion to a Y-shaped dispersion have been observed upon photon energy variation or by changing the Brillouin zone (BZ). Thereupon a combination of extrinsic and intrinsic effects have been invoked to explain the ARPES results of cuprates at high energies [11, 13, 33].

In this Letter we address the controversy of the explanation of the HEA in terms of extrinsic or intrinsic effects. We present a polarization and photon energy dependent ARPES study on the electron-doped cuprate [34] $\text{Nd}_{2-x}\text{Ce}_x\text{CuO}_4$ ($x = 0.123$) in several BZs. We find that the waterfall-like dispersion transforms into a normal, dispersive band at certain photon energies. In addition, a waterfall-like dispersion can be induced in the intact band by changing the polarization of the incoming photons. The results can be explained in terms of a wipe-out of the intensity of the broadened quasi-particle band in a particular momentum range. Thus we give strong evidence that the HEA is not caused by intrinsic many-body effects but rather by extrinsic matrix element effects. Furthermore, the newfound ability to observe the dispersion in the entire BZ allows us to determine the mass renormalization of the quasi-particle band relative to density functional theory (DFT) calculations.

The $\text{Nd}_{2-x}\text{Ce}_x\text{CuO}_4$ ($x = 0.123$) single crystal was grown in about 4 atm of oxygen using the traveling-solvent floating-zone technique, annealed for 10 h in argon at 970 °C followed by 20 h in oxygen at 500 °C [35]. The sample was antiferromagnetic with a Néel temperature of about $T_N = 82$ K [36]. ARPES measurements were carried out at the synchrotron radiation facility BESSY II using the UE112-PGM2a variable photon polarization beam line and the "I²"-ARPES end station equipped with a Scienta R8000 analyzer. All measurements were performed in the normal state at $T = 50$ K. The total energy resolution was set between 10 and 15 meV, while the angular resolution was $\approx 0.2^\circ$. We point out that the ARPES experiments were performed at relatively high photon energies ($h\nu = 50$ to 120 eV), a range in which the cross section for Cu $3d$ state excitations is 5 to 7 times larger than that for O $2p$ states [37]. The crystal was mounted on a 6-axis cryomanipulator allowing polar, azimuthal, and tilt rotation of the sample in ultrahigh vacuum with a precision of 0.1° . The experimental geometry is shown in Fig. 1(a). The mirror plane $(0, 0, \pi) - \Gamma - (\pi, 0, 0) \hat{=} (x, 0, z)$ was turned into the scattering plane. In this way cuts shown in Fig. 1(b) parallel to the $\Gamma - (0, \pi)$ direction for various k_x values could be

recorded by changing the polar angle from nearly normal incidence to more grazing incidence. In the chosen sample orientation, the Cu $3d_{x^2-y^2}$ conduction band states have an even symmetry with respect to the scattering plane as shown in Fig. 1(a). For non-zero photoemission intensity on the mirror plane, the final state must be even with respect to this plane and the same holds for the product of the dipole operator and the initial state. Therefore, for this sample orientation and for p -polarized light (\mathbf{e} parallel to the mirror plane, dipole operator even) the matrix element should be finite near the mirror plane, while for s -polarized light (\mathbf{e} perpendicular to the mirror plane, dipole operator odd) the matrix element should vanish (see Eq. 2). In a study of the origin of the shadow Fermi surface in cuprates it was shown that the intensity vanishes in a narrow range of $\pm 2^\circ$ when the transition is symmetry forbidden [38].

ARPES intensity calculations were done fully relativistically based on the Dirac equation [39]. One-step model [40] and multiple scattering theory have been utilized, the latter being used also for the final states. The potential for Nd_2CuO_4 has been calculated by using self-consistent electronic structure calculations with the Korringa-Kohn-Rostoker method [41, 42]. In the calculations, many-body correlations were taken into account by the complex self-energy function Σ . For the initial state we used the experimental self-energy function derived from the ARPES experiments (see below). For the final state a constant value $\Im\Sigma_f = 2$ eV is used.

In Fig. 1(c) and (d) we present the sum of ARPES intensity plots along the edges of the BZ recorded with right (c_+) and left (c_-) circularly polarized photons having two different photon energies. For $h\nu = 120$ eV [see Fig. 1(c)] and $k_x = 5\pi$ [cut#3 in Fig. 1(b)] a clear HEA at $E_H = 0.25$ eV is detected. At this energy the normal dispersion transforms into a vertical waterfall-like dispersion accompanied by a reduction of the intensity near $k_y = 0$. On the other hand, changing the photon energy to $h\nu = 94$ eV [see Fig. 1(d)] and $k_x = \pi$ [cut#2 in Fig. 1(b)] transforms the dispersive feature into a band having a normal dispersion with a width at constant energy which increases continuously with increasing binding energy. Since we observe similar changes as a function of photon energy for $k_x = n\pi$ $n = 1, 3$, and 5 (not shown) we conclude that the change of the spectra shown in Fig. 1(c) and (d) is caused by the variation of the photon energy but not by the change of k_x . Furthermore, $\text{Nd}_{2-x}\text{Ce}_x\text{CuO}_4$ is essentially a two-dimensional electronic system [43] and therefore upon variation the photon energy k_\perp changes, but this should not change the spectral function. Thus the drastic change of the intensity plots presented in Fig. 1(c) and (d) signals that the HEA is caused by matrix element effects but not by changes of the spectral function.

In Fig. 1 (e)-(g) we present similar energy distribution maps but now recorded with the wave vectors $k_x = \frac{3\pi}{8}$

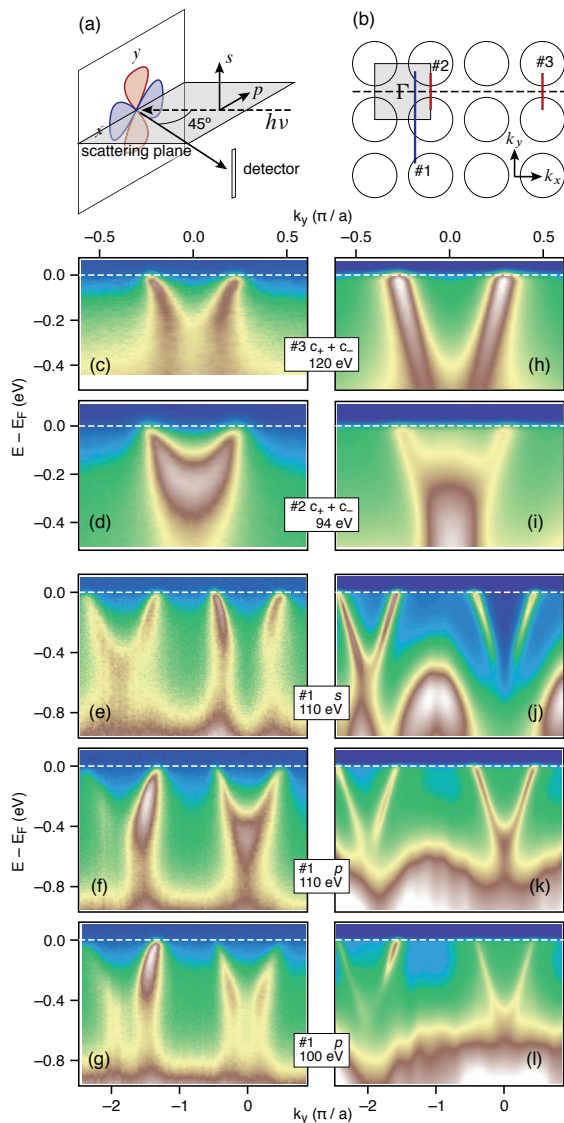


Figure 1. (Color online) (a) Experimental geometry. (b) Cuts in the reciprocal space used in the present investigation. (c) Experimental ARPES intensity distribution maps recorded with parameters given in the labels. (h)-(l) calculated ARPES intensities using the parameters of (c)-(g), respectively.

[cut#1 in Fig. 1(b)]. In these cuts we cross the Fermi surface at the nodal point. For $h\nu = 110$ eV and p -polarization, near $k_y = 0$ a normal dispersion is observed [see Fig. 1(f)]. Compared to the antinodal point, the bottom of the band has moved to higher E_B , which is expected from band structure calculations. The spectral weight of the band extends into the region of the non-bonding oxygen valence bands. On the other hand, near $k_y = -2\pi$, a HEA is observed. At the same photon energy ($h\nu = 110$ eV) but for s -polarization, we know that the intensity must vanish at the mirror plane ($k_y = 0$). In Fig. 1(e) we see that, when the matrix element is intentionally suppressed in this way, a HEA appears at

$E_H = 0.4$ eV. Thus the existence of the waterfall-like dispersion can be unambiguously attributed to a vanishing matrix element near $k_y = 0$. In the second BZ we detect a more normal dispersion. Furthermore, for the photon energy $h\nu = 100$ eV but for p -polarization, a HEA is observed in the first and the second BZ [see Fig. 1(g)]. Comparing the spectra presented in Fig. 1(f) and (g) which were measured both with the same (p) polarization, the difference near $k_y = 0$ cannot be explained by an extinction of the matrix element due to a specific photon polarization but by an extinction of the matrix element near the $(k_x, k_y = 0)$ line for specific photon energies. Comparing the intensities near $k_y = 0$ presented in Fig. 1(e) and (g), it is remarkable that the distances between the waterfall-like dispersions in momentum space along k_y is in the former about twice as large as in the latter. We attribute the differences in the energies E_H (changing from 0.4 eV to 0.55 eV) to the different extinction ranges of the matrix elements. In Fig. 2(a) we plot the bottom of the band along the $\Gamma - (\pi, 0)$ direction, derived from fits of energy distribution curves at $k_y = 0$ using spectra showing no HEA and compare this result with our density function theory (DFT) calculations.

The interpretation of the ARPES results on the HEA in terms of matrix element effects is supported by a simple calculation of the matrix element for the selected geometry and sample orientation using atomic wave functions for the $|d\rangle$ initial state and $\langle p| / \langle f|$ final states [44]. As expected from the discussion above, these calculations yield for s -polarization a vanishing matrix element at the mirror plane, but for photons emitted at a finite angle relative to the mirror plane the matrix element increases linearly with that angle. This means that for small angles the intensity should increase proportional to k_y^2 which is in perfect agreement with a momentum distribution curve at $E_B = 0.5$ eV of the ARPES data shown in Fig. 1(e) [see Fig. 2(b)]. One explanation to account for the observed $h\nu$ -dependence would be that for particular photon energies only final states which are odd with respect to the mirror plane can be reached. This would explain why for p -polarization the intensity is zero in the mirror plane. The calculation predicts for finite emission angles relative to the mirror plane a finite intensity proportional to k_y^2 due to even final states which contribute to the matrix element linearly with increasing angle. This would explain why for certain energies even for p -polarization a waterfall-like dispersion is observed [see Fig. 1(g)].

The interpretation of the HEA in terms of extrinsic matrix element effects is furthermore strongly supported by the ARPES intensity calculations which are in qualitative agreement with the experimental ARPES data [see Fig. 1(h)-(l)]. Part of the remaining differences are related to the fact that for the non-bonding O $2p$ bands, the same self-energy function as for the Cu $3d$ band has been used which leads to an unphysical broadening of the

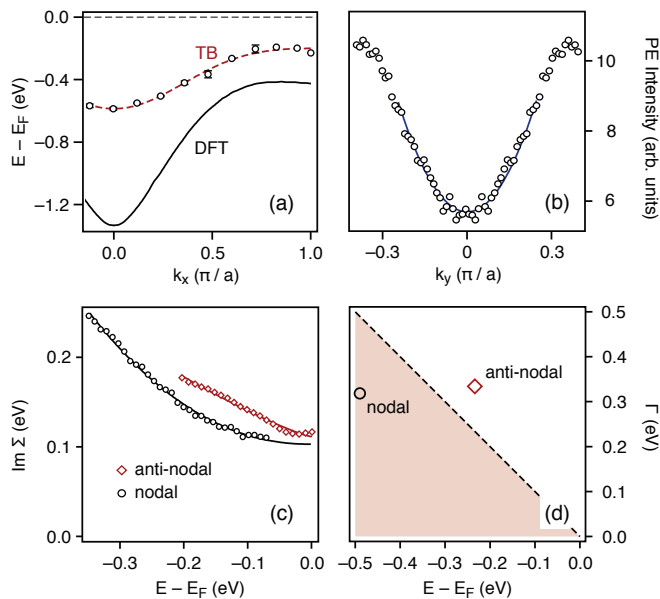


Figure 2. (Color online) (a) Bottom of the band along the $(-\pi,0)$ - $(\pi,0)$ direction between the center of the BZ and the antinodal point. Circles: ARPES data. Dashed line: tight binding (TB) fit. Solid line: present density functional theory (DFT) calculations. (b) Momentum distribution curve of the data shown in Fig. 1(e) at $E_B = 0.5$ eV, symmetrized relative to $k_y = 0$. The blue line shows a quadratic momentum dependence. (c) Imaginary part of the self-energy $\Im\Sigma$ as a function of the binding energy near the nodal and the antinodal point. The lines are fits to the data (see text). (d) Width Γ of the spectral weight at the bottom of the band near the antinodal point [$k_{\parallel} = (\pi, 0)$] and at the cut through the nodal point [$k_{\parallel} = (\frac{3\pi}{8}, 0)$]. Red region indicates the range of the existence of quasi-particles ($\Gamma < E_B$).

former bands.

The presented ARPES data together with the supporting calculations provide strong evidence that the HEA is not related to an anomalous spectral function, i.e., to specific many-body effects. Rather, it is caused by a wipe-out of a broad intensity distribution of the spectral weight near particular high-symmetry lines due to the extinction of the matrix elements (see also Fig. 2 in the supplement [44]), i.e., by extrinsic effects. We point out that the formation of a waterfalllike dispersion requires both a vanishing matrix element and a strong broadening of the spectral weight at higher binding energies. This explains why the HEA has only been found in strongly correlated systems in which a strong broadening of the "bands" at higher binding energies due to high scattering rates is present.

The present work can explain various results presented in the literature which were not understood previously. For example, the momentum dependence of E_H , when going from the nodal to the antinodal point, previously observed in $\text{La}_{2-x}\text{Sr}_x\text{CuO}_4$ [6] and $\text{Nd}_{2-x}\text{Ce}_x\text{CuO}_4$ [14] can be readily explained in terms of a wipe-out of the

intensity of a normal quasi-particle band, in which the bottom of the band near Γ is deeper than near the antinodal point. Furthermore, the difference of the E_H values of ≈ 0.4 eV between p - and n -doped cuprates, which was linked to the difference of the chemical potential [14] can be now understood by a wipe-out of quasi-particle bands, ranging to different energies below the Fermi level.

Since we can now follow the dispersion to the bottom of the band, we can derive reliable results for the mass enhancement compared to DFT calculations. Using the data presented in Fig. 2(a), we obtain a high-energy mass renormalization of 2.1 near the antinodal point while at Γ a value of 2.3 derived. We remark that these values are connected with large errors of about 30% since there is a considerable scattering of the energy position of the Cu-O conduction band relative to the Fermi level in the published DFT calculations. Moreover, we have analyzed the energy-dependence of the imaginary part of the self-energy, extracted from momentum distribution curves, using the relation $\Im\Sigma = -A - BE^\alpha$ [see Fig 2(c)]. Near the antinodal point we obtain $A = 0.111 \pm 0.003$ eV, $B = 0.47 \pm 0.09$ eV $^{1-\alpha}$ and $\alpha = 1.2 \pm 0.1$, while near the nodal point $A = 0.103 \pm 0.002$ eV, $B = 1.4 \pm 0.1$ eV $^{1-\alpha}$, and $\alpha = 2.15 \pm 0.07$. The observation of a nearly quadratic increase as a function of energy at the nodal point indicates a Fermi liquid behavior and explains the quadratic temperature dependence of the in-plane resistivity above the superconducting transition temperature [45]. The nearly linear increase at the antinodal point signals the proximity to a marginal Fermi liquid [46]. Near the center of the BZ, at $k_{\parallel} = (\frac{3\pi}{8}, 0)$ the total life-time broadening amounts to 65 % of E_B [see Fig. 2(d)]. This indicates that even at the bottom of the band, spectral weight of quasi-particles is observed and that at these E_B s we are not in the incoherent range as suggested previously in the literature [5, 18, 21, 26, 32]. In addition, the lack of a high-energy kink and the continuous increase of the width as a function of E_B do not support any scenario of a strong coupling of the charge carriers to discrete high-energy bosonic excitations such as magnetic excitations with an energy of $2J \approx 0.3$ eV (J is the exchange energy) [34] which could mediate high- T_c superconductivity [9, 17, 19, 29, 33]. Rather, the results presented here indicate a strong coupling of the charge carriers to low-energy electronic excitations, e.g. spin excitations between regions near the antinodal points leading there to a marginal Fermi liquid behavior as described by [47, 48]. Finally, we postulate that the present results can be generalized to all cuprates since in the p -doped compounds very similar ARPES results, e.g. energy dependence of E_H , have been obtained [6].

To summarize, our ARPES results on an n -doped cuprate together with a calculation of the ARPES intensity in a one-step model clearly show that the HEA is not related to an intrinsic anomalous dispersion of the spectral weight. Rather, it is exclusively caused by a combina-

tion of a wipe-out due to matrix element effects and high scattering rates at high energies. By selecting suitable photon energies we are able to obtain important information on the many-body properties of doped cuprates which places strong constraints on theories of high- T_c superconductivity in these systems. Furthermore, the present results provide important information about the electronic structure of doped Mott-Hubbard insulators: a vertical dispersion between the coherent quasi-particles and the incoherent lower Hubbard band [5, 18, 21, 26, 32] is not supported.

We thank Inna Vishik for valuable comments. The work at the University of Minnesota was supported by the NSF and the NSF MRSEC program.

-
- [1] A. Damascelli, Z. Hussain, and Z.-X. Shen, *Rev. Mod. Phys.* **75**, 473 (2003).
- [2] J. Graf et al., *Phys. Rev. Lett.* **98**, 067004 (2007).
- [3] F. Ronning et al., *Phys. Rev. B* **71**, 094518 (2005).
- [4] Z. Pan et al., eprint arXiv:cond-mat/0610442 (2006).
- [5] W. Meevasana et al., *Phys. Rev. B* **75**, 174506 (2007).
- [6] J. Chang et al., *Phys. Rev. B* **75**, 224508 (2007).
- [7] B. P. Xie et al., *Phys. Rev. Lett.* **98**, 147001 (2007).
- [8] D. S. Inosov et al., *Phys. Rev. Lett.* **99**, 237002 (2007).
- [9] T. Valla et al., *Phys. Rev. Lett.* **98**, 167003 (2007).
- [10] D. S. Inosov et al., *Phys. Rev. B* **77**, 212504 (2008).
- [11] W. Meevasana et al., *Phys. Rev. B* **77**, 104506 (2008).
- [12] W. Zhang et al., *Phys. Rev. Lett.* **101**, 017002 (2008).
- [13] B. Moritz et al., *New J. Phys.* **11**, 093020 (2009).
- [14] M. Ikeda et al., *Phys. Rev. B* **80**, 184506 (2009).
- [15] F. Schmitt et al., *Phys. Rev. B* **83**, 195123 (2011).
- [16] R. S. Markiewicz and A. Bansil, *Phys. Rev. B* **75**, 020508 (2007).
- [17] R. S. Markiewicz, S. Sahrakorpi, and A. Bansil, *Phys. Rev. B* **76**, 174514 (2007).
- [18] K. Byczuk et al., *Nat Phys* **3**, 168 (2007).
- [19] A. Macridin, M. Jarrell, T. Maier, and D. J. Scalapino, *Phys. Rev. Lett.* **99**, 237001 (2007).
- [20] P. Srivastava, S. Ghosh, and A. Singh, *Phys. Rev. B* **76**, 184435 (2007).
- [21] F. Tan, Y. Wan, and Q.-H. Wang, *Phys. Rev. B* **76**, 054505 (2007).
- [22] R. G. Leigh, P. Phillips, and T.-P. Choy, *Phys. Rev. Lett.* **99**, 046404 (2007).
- [23] L. Zhu, V. Aji, A. Shekhter, and C. M. Varma, *Phys. Rev. Lett.* **100**, 057001 (2008).
- [24] P. Wrobel, W. Suleja, and R. Eder, *Phys. Rev. B* **78**, 064501 (2008).
- [25] C. Weber, K. Haule, and G. Kotliar, *Phys. Rev. B* **78**, 134519 (2008).
- [26] M. M. Zemljic, P. Prelovsek, and T. Tohyama, *Phys. Rev. Lett.* **100**, 036402 (2008).
- [27] K. Matho, *J. Electron Spectrosc.* **181**, 2 (2010).
- [28] S. Sakai, Y. Motome, and M. Imada, *Phys. Rev. B* **82**, 134505 (2010).
- [29] R. Markiewicz, T. Das, S. Basak, and A. Bansil, *J. Electron Spectrosc.* **181**, 23 (2010).
- [30] B. Moritz, S. Johnston, and T. Devereaux, *J. Electron Spectrosc.* **181**, 31 (2010).
- [31] D. Katagiri, K. Seki, R. Eder, and Y. Ohta, *Phys. Rev. B* **83**, 165124 (2011).
- [32] E. Manousakis, *Phys. Rev. B* **75**, 035106 (2007).
- [33] S. Basak et al., *Phys. Rev. B* **80**, 214520 (2009).
- [34] N. P. Armitage, P. Fournier, and R. L. Greene, *Rev. Mod. Phys.* **82**, 2421 (2010).
- [35] P. K. Mang et al., *Phys. Rev. B* **70**, 094507 (2004).
- [36] E. M. Motoyama et al., *Nature* **445**, 186 (2007).
- [37] J. Yeh and I. Lindau, *At. Data Nucl. Data Tables* **32**, 1 (1985).
- [38] A. Mans et al., *Phys. Rev. Lett.* **96**, 107007 (2006).
- [39] J. Braun, *Rep. Progr. Phys.* **59**, 1267 (1996).
- [40] J. Pendry, *Surf. Sci.* **57**, 679 (1976).
- [41] S. Kaprzyk and A. Bansil, *Phys. Rev. B* **42**, 7358 (1990).
- [42] A. Bansil, S. Kaprzyk, P. E. Mijnarends, and J. Toboła, *Phys. Rev. B* **60**, 13396 (1999).
- [43] S. Massidda, N. Hamada, J. Yu, and A. Freeman, *Physica C* **157**, 571 (1989).
- [44] see information presented in the Supplement.
- [45] C. Tsuei, A. Gupta, and G. Koren, *Physica C* **161**, 415 (1989).
- [46] C. Varma, Z. Nussinov, and W. van Saarloos, *Physics Reports* **361**, 267 (2002).
- [47] P. Monthoux, A. V. Balatsky, and D. Pines, *Phys. Rev. Lett.* **67**, 3448 (1991).
- [48] A. Abanov, A. V. Chubukov, and J. Schmalian, *Adv. Phys.* **52**, 119 (2003).

Supplementary material for: The high-energy anomaly in ARPES spectra of the cuprates—many body or matrix element effect?

E. D. L. Rienks,¹ M. Ärrälä,² M. Lindroos,² F. Roth,³ W. Tabis,^{4,5} G. Yu,⁴ M. Greven,⁴ and J. Fink⁶

¹Helmholtz-Zentrum Berlin, Albert-Einstein-Strasse 15, D-12489 Berlin, Germany

²Department of Physics, Tampere University of Technology, PO Box 692, FIN-33101 Tampere, Finland

³Center for Free-Electron Laser Science / DESY, Notkestrasse 85, D-22607 Hamburg, Germany

⁴School of Physics and Astronomy, University of Minnesota, Minneapolis, Minnesota 55455, USA

⁵University of Science and Technology, Faculty of Physics and Applied Computer Science, 30-059 Krakow, Poland

⁶Leibniz-Institute for Solid State and Materials Research Dresden, P.O.Box 270116, D-01171 Dresden, Germany

In this supplement, we provide angle-dependent calculations of the matrix element for photoemission experiments described in the main paper using atomic orbitals for the Cu $3d$ initial and the dipole allowed Cu $2p$ or $4f$ final states. When the matrix element is symmetry-forbidden on the mirror plane, it is found to increase linearly with increasing emission angle relative to this plane. Thus the ARPES intensity should increase quadratically with the distance k_y from the mirror plane. This explains the wipe-out near the $x-z$ plane for s -polarization and thus the waterfalllike dispersion.

PACS numbers: 74.25.Jb, 74.72.Ek, 79.60.i

In ARPES the measured photocurrent is given by

$$I(\omega, \mathbf{k}) \propto |M(\omega, \mathbf{k})|^2 A(\omega, \mathbf{k}) \quad (1)$$

where $A(\omega, \mathbf{k})$ is the spectral function and the matrix element

$$M(\omega, \mathbf{k}) = \langle f | \mathbf{e} \mathbf{r} | i \rangle \quad (2)$$

is determined by the final state $\langle f |$, the initial state $|i\rangle$, and the dipole operator $\mathbf{e} \mathbf{r}$ (\mathbf{e} is the unit vector along the polarization direction of the photons) [1]. In the following we calculate the matrix elements for the geometry and sample orientation described in the main paper using atomic initial and final states. The dipole operator for s - and p -polarization is proportional to a linear combination of Θ and φ dependent spherical harmonics by $Y_1^1 - Y_1^{-1} \propto \sin(\Theta)$ and $Y_1^1 + Y_1^{-1} \propto \cos(\Theta)$, respectively. Θ denotes the angle in the $z-y$ plane perpendicular to the mirror plane, while φ is the angle around the z axis. The Θ -dependence of the matrix element is given by the relation

$$M(f, i, \Theta) \propto \int_0^\pi Y_{l_f}^{m_f} (Y_1^1 \pm Y_1^{-1}) Y_{l_i}^{m_i} \sin \theta d\theta \quad (3)$$

The initial state is a Cu $3d_{x^2-y^2}$ state, hence the initial state is determined by $l = 2, m = \pm 2$ and therefore $\langle i | \propto Y_2^{\pm 2} \propto \sin^2(\theta)$. According to the dipole selection rules $\Delta l = \pm 1$ and $\Delta m = 0, \pm 1$ excitations into $\langle p |$ and $\langle f |$ final states can occur. In the case of p -polarization allowed final states are $Y_1^{\pm 1} \propto \sin(\theta)$ which is even with respect to the mirror plane. For p -polarization (even dipole operator) the matrix element is finite since both the initial and the final states are even. On the other hand, for s -polarization (odd dipole operator) the matrix element vanishes since both the initial state and the final state are even. In this case when the emitted photons

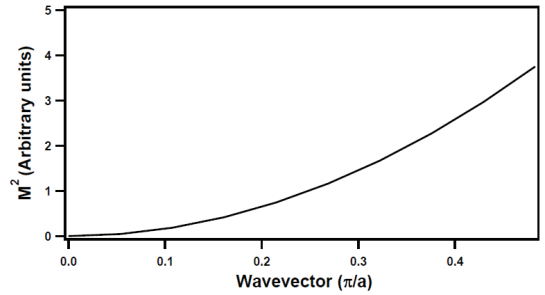


Figure 1. Calculated squared matrix element M^2 versus the wave vector k_y perpendicular to the mirror plane.

have a small angle δ versus the mirror plane, the final states are proportional to $\sin(\Theta + \delta) \approx \sin(\Theta) + \delta \cos(\Theta)$. The second term now adds an odd contribution to the final state and we will have a finite matrix element which is proportional to δ . Thus for small δ the intensity is $I(\delta) \propto M^2 \propto \delta^2 \propto k_y^2$. In Fig.1 we show the calculated squared matrix element M^2 versus k_y . A similar calculation for transitions into $\langle f |$ final states results in a matrix element which is also proportional to k_y .

In Fig. 2(d) of the main paper we show the intensity along k_y from a momentum distribution curve at a binding energy of 0.5 eV of the ARPES intensity distribution map shown in Fig. 1(e) of the main paper. At small k_y the intensity agrees perfectly with a quadratic dependence on k_y indicating that the appearance of the waterfalllike dispersion can be explained in terms of a simple calculation of the matrix element using atomic initial and final state wave functions.

In Fig. 2(a) we show the calculated intensity derived from a spectral function using for convenience a parabolic band and a complex self-energy function [which shows no

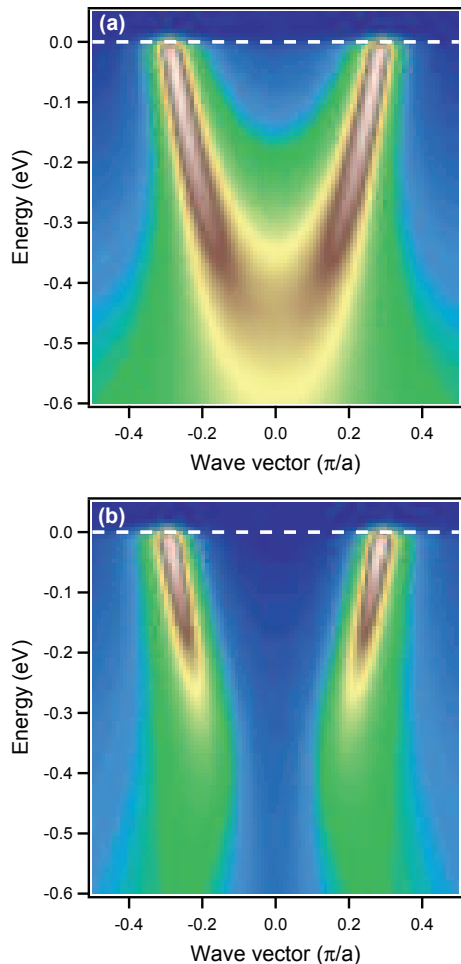


Figure 2. (Color online) (a) Calculated ARPES intensity distribution map using a parabolic band together with a self-energy without a high-energy anomaly derived from the experiment. (b) The same intensity distribution map as in (a) but multiplied by a matrix element which is quadratic in the wave vector. A waterfalllike dispersion is produced.

high-energy anomaly (HEA)] taken from the experiment

at the nodal point which was mentioned in the main paper. A Shirley background [2] was added. Multiplying the spectral function with a matrix element which is proportional to k_y^2 we obtain the intensity distribution map shown in Fig. 2(b) which shows a HEA. This represents a further indication that the waterfall like dispersion is caused by matrix element effects.

Finally we discuss the energy dependence of the ARPES intensity for p -polarized photons using the present calculation of the matrix element [see Fig. 1(f) and (g) in the main paper]. If the final state is even and thus proportional to $\sin\Theta$ the three terms of in the integral over θ are even and thus the matrix element is finite yielding a normal dispersion without HEA. Upon changing the photon energy, at particular energies predominantly odd final states could be reached which are proportional to $\cos\Theta$. One explanation to account for the observed $h\nu$ dependence would be that for particular photon energies only odd final states are reached. Then for p -polarized photons and photoelectrons emitted in the mirror plane the matrix element is zero. Detecting electrons which are emitted at a small angle δ relative to the mirror plane, the final state is now proportional to $\cos(\Theta + \delta) \approx \cos\theta + \delta\sin\theta$. The second term yields an even contribution to the final state proportional to δ . Thus the finite matrix element increases proportional to δ and the intensity proportional to δ^2 causing a HEA similar to the case for s -polarized photons. In this way it is possible to explain the energy dependence of the ARPES intensity, shown in Fig. 1(f) and (g) in the main paper, by an energy dependent change of the parity of the final states.

-
- [1] A. Damascelli, Z. Hussain, and Z.-X. Shen, Rev. Mod. Phys. **75**, 473 (2003).
 [2] D. A. Shirley, Phys. Rev. B **5**, 4709 (1972).